Transparent elongation and compressive strain sensors based on aligned carbon nanowalls embedded in polyurethane

Transparent elongation and compressive strain sensors based on aligned carbon nanowalls embedded in polyurethane

Petr Slobodian[a b *], Pavel Riha[c], Hiroki Kondo[d], Uros Cvelbar[e], Robert Olejnik[a], Jiri Matyas[a], Makoto Sekine[d], Masaru Hori[d]

[a] *Centre of Polymer Systems, University Institute, Tomas Bata University, Tr. T. Bati 5678, 760 01, Zlín, Czech Republic*

[b] *Tomas Bata University, Faculty of Technology, Polymer Centre, T.G.M. 275, 760 01, Zlin, Czech Republic*

[c] *The Czech Academy of Sciences, Institute of Hydrodynamics, Pod Patankou 5, 166 12, Prague 6, Czech Republic*

[d] *Plasma Nanotechnology Research Center (PLANT), Graduate School of Engineering, Nagoya University, Furo-cho Chikusa-ku, Nagoya, 464-8603, Japan*

[e] *Jozef Stefan Institute, Department F6, Jamova cesta 39, SI-1000, Ljubjana, Slovenia*

** Corresponding author at: Centre of Polymer Systems, University Institute, Toma: Bata University, Tr. T. Bati 5678, 760 01, Zlin, Czech Republic. E-mail address: slobodian@ft.utb.cz (P. Slobodian).*

ABSTRACT

Highly extensible transparent composite materials comprised of maze-like vertically aligned carbon nanowalls embedded perpendicularly into a polyurethane film were used as strain tensors and tested by an electrical resistance method in the course of extension, extension/relaxation and compression/expansion cycles. The maze-like carbon nanowall networks with wall-to-wall average distances of 100,200 and 300 nm were formed on SiO_2-coated Si substrates by a plasma-enhanced chemical vapor deposition system. Afterwards, the nanowall network was embedded into a stretchable polyurethane matrix which enabled a high deformation of the composite. The measured extensibility of the composite was over 440 %, and its resistance increased with the extension. The sensitivity of the detection of extension, which was evaluated by the gauge factor, increased over 2000. These sensor properties can be readily tuned by varying distances of nanowalls within the network. Finally, thanks to their optical transparency in the visible light region and thermoelectric properties, these composites offer a wide range of further practical applications.

Keywords: Carbon nanowalls, Polyurethane substrate, Deformation, Thermoelectric properties

1. Introduction

Carbon nanowalls (CNWs), 2-D nanostructures made of several graphene sheets stacked over each other, possess multiple exceptional properties, which make them valuable in various applications, for example, as CNW based electro-mechanical, electro-chemical and wearable temperature sensors **[1-4]**, biosensors **[5,6]**, electrochemical transducers **[7]**, fuel cell components **[8]**, stretchable electronic skin **[9]**, etc. CNWs are grown on flat substrates using various plasma-enhanced chemical vapor deposition methods. The resulting self-organized multilayered carbon nanowalls with preferred

vertical orientation and with CNW thickness in the range from a few nanometers to a few tens of nanometers comprise of a constantly decreasing number of graphene layers in the direction of growth, which terminates into extremely sharp edges on top **[10]**. The number of CNWs per unit length can be successfully controlled by varying processing parameters, such as the total pressure and the discharge power during the growth of CNWs **[11]**. The final CNW structure is an inter-connected and self-supported three-dimensional tangled network **[11-14]**. The CNW network is electrically conductive. Its conductivity is mainly affected by the resistance of contacts between individual graphene sheets forming the carbon nanowall and by the contact resistance of the nanowall junctions **[11,15]**. Consequently, the detection mechanisms of CNW networks are determined by various modulations of these contacts, which subsequently affect the total contact resistance of CNW. For example, vapors of volatile organic compounds substantially enhance the contact resistance of CNWs by the formation of non-conducting layers in the contacts between both the individual graphene sheets and the respective CNWs **[16]**. Similarly, when the CNW network is subjected to a compression, the principle of load sensing by the CNWs is similarly a change of their contact resistance **[17]** or a formation of microcracks in the conductive CNW network **[1]**.

Strain sensors based on a unique structure of a vertical network of CNWs embedded in polydimethylsiloxane are exceptionally stretchable up to about 130 % when the CNWs are approximately 2 μm high **[1].**

Table 1 Manufacturing data and the average height of CNWs with the average distances between them 100, 200 and 300 nm.

Average distance between CNTs [nm]	100	200	300
Thickness of SiO_2 coating on Si substrate [nm]	100	10	1
Average height of CNWs [nm]	650	1000	970
Electrical conductivity [S/cm]	38	49	76
Process pressure [Pa]	1	5	5
Substrate temperature [°C]	600	600	600
SWP power [W]	400	400	400
CCP power [W]	100	400	500
H_2[sccm]:CH_4[sccm]	50:100	50:100	50:100
Growth time [min]	60	29	10

However, when the embedded CNWs are taller, the ultimate strain is lower, and the composite is less stretchable. Therefore, the strain sensitivity can be tuned by using CNWs of a different height and thickness. Moreover, our data on the sensitivity of CNW-based sensors for detection of organic vapors **[16]** show that wall-to-wall distances also influence the electrical response to ambient vapor. The significance of this wall spacing for vapor sensing suggests its possible role in the detection of strain in extension and compression of a substrate with embedded CNWs. To test this hypothesis, we used a novel sensor consisting of CNWs embedded in polyurethane and assessed its response to various deformations as well as its other properties such as the thermoelectricity and light transparency.

2. Experimental

2.1. Materials

The carbon nanowalls were fabricated using a capacitively coupled microwave radio- frequency plasma-enhanced chemical vapor deposition assisted by an H radical injection and grown on a SiO_2-coated Si substrate (in further text layered substrate). The uniqueness of the fabrication was that H

and CH radical density were separately controlled in two plasma regions. The surface wave plasma region with a 2.45 GHz microwave power supply, generated H radicals and capacitively coupled plasma (CCP) region generated by a 100 MHz power supply fabricated nanowalls from CH_4 gas, **Fig. 1**. Variation of experimental conditions led to different average distances between adjacent CNWs as well as varying CNW average heights, as summarized in **Table 1**.

Grown CNWs were transferred from the layered substrate to a stretchable thermoplastic polyurethane (TPU) Desmopan DP 385S (Bayer MaterialScience). The ultimate strength of TPU of 48.9 MPa, with the strain at break 442.2 % and density of 1.20 g/cm^3 were specified by the supplier. To replace the rigid technological layered substrate with an elastic one, the following procedure was employed: TPU was dissolved in dimethyl formamide (DMF) to get a 5 wt% solution. Then the network of vertically grown CNWs on the layered substrate was partly infused with the DMF/TPU solution (~1.8ml/cm^2) and dried at room temperature for 24 h. The filling with the same amount of the DMF/TPU solution and subsequent drying for 24 h was repeated once. Afterwards, the layered substrate with the CNW/TPU composite layer (Si layer of the substrate on top) of the size 10 x 30 mm was subsequently attached by compression (75 kPa) to a TPU dog-bone shaped tensile specimen. The tensile specimen was 2 mm thick and made by compression molding from Desmopan DP 385S. The shape and dimensions of the sample were chosen according to the standard EN ISO 3167. Ultimately, the upper technological layered substrate was peeled off.

The multi-walled carbon nanotubes (MWCNTs) were used to compare their strain sensing ability with the CNW/TPU sensors. MWCNTs, which were produced by the acetylene chemical vapor deposition method (purity >90 %), were purchased from Sun Nanotech Co. Ltd.

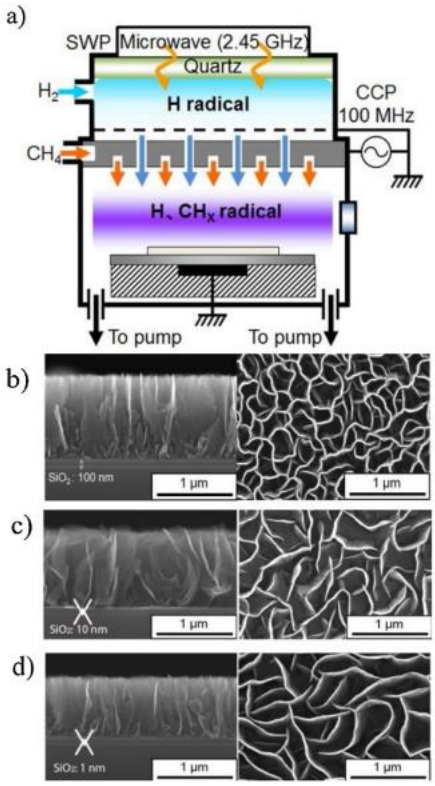

Fig. 1. a) Schematic diagram of the plasma-enhanced chemical vapor deposition technique used for the growth of CNWs. SEM micrographs depicting cross-sections and upper surfaces of CNWs with the average wall distances of 100,200 and 300 nm grown on a layered substrate with SiO_2-coating layer of 100, 10,1 nm (panels b, c and d), respectively.

Further details on the nanotubes were obtained by transmission electron microscopy and described in our previous papers **[18,19]**. The diameter of individual nanotubes was determined from the corresponding micrographs to be between 10 and 60 nm, their length from tenths of micrometers up to 3 μm. The maximum aspect ratio of the nanotubes was about 300.

2.2. Measurement of the composite tensile and compressive deformation

The change of the electrical resistance of the CNW/TPU composite, used as an electromechanical sensor attached to the dog-bone shaped tensile specimen in the course of tensile tests, was measured lengthwise by a two-point technique using the multimeter Sefram 7338, which was storing the results once per second. A screw was used for the attachment of two copper electrodes to the tested composite.

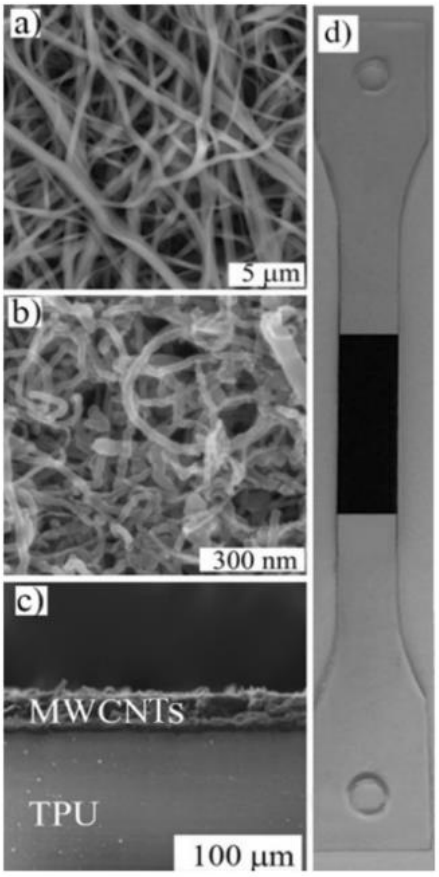

Fig. 2. a) SEM micrograph of the polyurethane non-woven filtering membrane, b) SEM micrograph of the filter cake surface formed by entangled pristine MWCNTs, c) MWCNT composite cross-section after the melt welding (the thickness of the MWCNT layerembedded into TPU was 35 μm), d) the photograph ofTPU dog-bone shaped specimen for the tensile test with the fixed stripe ofMWCNT/TPU composite (black strip).

The screw tightening was terminated when there was no decrease in the CNW network resistance. In that manner, the contact resistance between CNWs and copper electrodes was controlled, and the initial electrical resistance of the system was equally adjusted before the elongation of the first sample.

Faster loading events (strain cycles, vibration) were monitored by the Multiplex datalogger 34980A, which was storing the results with frequency 90 Hz.

The active sensory layer of the MWCNT/TPU strain sensor consisted of the entangled MWCNT network deposited on the TPU non-woven filtering membrane, **Fig. 2**a. The membrane with the MWCNT network (**Fig. 2**b, c) was melt welded (at 175 °C) onto the surface of the TPU dog-bone shaped tensile specimen used for the mechanical testing, **Fig. 2**d.

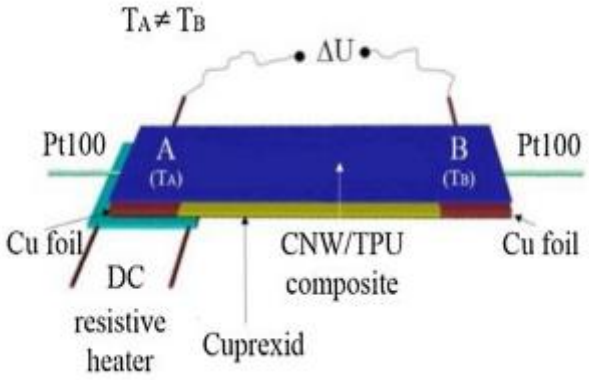

Fig. 3. Schematic diagram of the set up for the measurement of the voltage induced in the CNW/TPU composite in response to a temperature difference between the hot side A and the cold side B.

Change of the electrical resistance of the layered MWCNT/TPU composite sensor in the course of extension and extension/relaxation cycles was measured in a similar way as the above-described deformation of the CNW/TPU composite sensor.

The response of the sensor made of the CNW/TPU composite with an average nanowall distance 300 nm attached to a TPU strip (length 15 mm, width 10 mm and thickness 2 mm) was also tested during six compression/relaxation cycles. The composite sensor was at first stepwise compressed by a small steel plate with a pressing area 10 x 10 mm to the maximum value 177.2 kPa with a 60 s delay of the resistance change reading in each tensile stress step equal to 20.4, 38.3, 56.2, 71.2, 86.2,101.2, 116.2, 137.7, 159.2, 177.2 kPa. Then the down-stress curve was measured in the same manner. The change of the composite electric resistance was measured lengthwise by the two-point technique using the multimeter Sefram 7338 as described in the case of the extension measurements.

2.3. Thermoelectric power measurement

The thermoelectric power of a material, as induced by the Seebeck effect, is a measure of the magnitude of an induced thermoelectric voltage in a response to a temperature difference across that material. The thermoelectric power measurement was carried out for the CNW/TPU composites with the average wall distances 100 and 300 nm using a setup illustrated in **Fig. 3**. The schematic diagram shows the Cuprexit plate with two Cu foils on sides and the CNW/TPU composite attached to these foils. A DC resistance heating altered temperature of the hot side A relatively to the cold side B of the Cu-CNW/TPU thermocouple.

2.4. Measurement of the CNW/TPU composite transmittance

The transmittance of the CNW/TPU and MWCNT/TPU composites was measured using the Cary 300 UV-vis Spectrophotometer (Varian, Inc., USA). Specifically, a 2 mm thick TPU strip, a 500 nm thick CNW/TPU composite (average nanowall distance 300 nm) attached to the TPU strip (thickness of 0.35 mm and 2 mm) and a 2 mm thick MWCNT/TPU composite were tested.

3. Results

Three different specimens of CNWs were grown on a layered substrate with different thickness of SiO2 coating at different experimental conditions determined by the CCP region power supply, the process pressure and the growth time (see Section **2**), which resulted in an average wall spacing of 100, 200 or 300 nm.

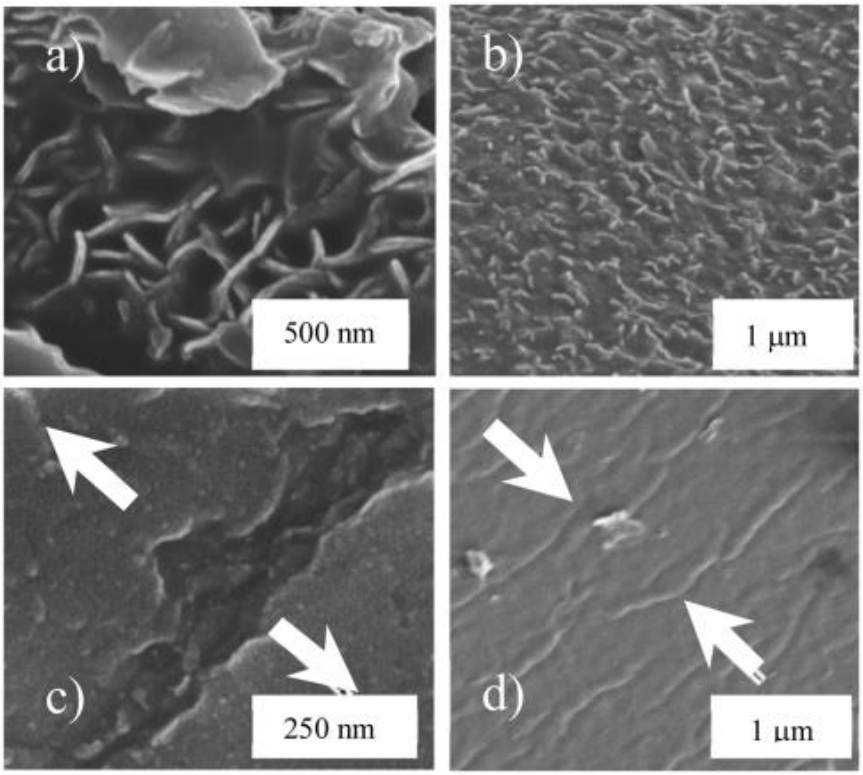

Fig. 4. SEM micrographs depicting the upper surface ofthe CNW/TPU composite (average wall distance 300 nm) with protruding carbon nanowalls, which was stripped from the layered substrate and etched with DMF to remove the surface part of the TPU matrix (panels a and b). SEM micrographs depicting the cracks in the upper surface of the CNW/TPU composite after an extension of 6.5 % (c) and relaxation (d). Arrows denote the direction of the extension and the compression of the sample.

These differences in nanowall spacing were visible in SEM micrographs of both the surface and the cross-sections of the maze-like nanowalls vertically grown on the layered substrate, **Fig. 1**b-d. The nanowall contacts enabled the electrical conductance as well as the compactness of the nanowall network.

Subsequently, the CNW/TPU composite prepared by the technique described in Section **2.1**.

was detached from the layered substrate and the surface part of the TPU matrix was etched off by DMS for 5 s. The protruding carbon nanowalls were clearly visible on the surface view of the etched composite (**Fig. 4**a, b).

The arrangement of nanowalls (average wall distance 300 nm) remained unchanged (**Fig. 4**a) after the space between the nanowalls was filled with polyurethane. No cracks were seen in the undeformed composite (**Fig. 4**b). The surface of the CNW/TPU composite after an extension of 6.5 % and a relaxation is shown in **Fig. 4**c, d. As follows from the extension and compression tests, the ensuing cracks increased the electrical resistance of the composite.

The photographs in **Fig. 5**a, b suggested partial transparency of the CNW/TPU composite in comparison with the MWCNT/TPU composite. Owing to the vertical orientation of the nanowalls, the light penetrated the CNW/TPU composite layer attached to the TPU strip. In contrast, the dense network of the interconnected carbon nanotubes ofthe MWCNT/TPU composite prevented the light from passing through the strip.

The results of the measured transmittance dependent on the wavelength of light are plotted in **Fig. 5**c. The MWCNT/TPU composite (thickness of about 2 mm) is not transparent (see also **Fig. 5**b). In contrast, the supporting TPU foil (thickness of 0.35 or 2 mm) did not substantially affect the transmittance of the CNW/TPU composite (average nanowall distance 300 nm). Consequently, CNW/TPU composites were transparent and could be used in applications, in which both the transparency and the other unique further described properties of this material would be required.

An effect of a tensile deformation on the resistance of the CNW/TPU (average nanowall distance 300 nm) and the MWCNT/TPU composite was assessed during five consecutive extension/relaxation cycles with an increasing strain in each cycle. In particular, the tensile stress increased stepwise in each cycle reaching 0.53, 1.58, 3.07, 5.44, 5.44MPa for the CNW/TPU composite and 0.50, 1.50, 2.92, 5.18, 5.18MPa for the MWCNT/TPU composite, **Fig. 6**. Resistance changes were defined as $\Delta R/R_0 = (R-R_0)/R_0$, where R_0 was the electrical resistance of the measured sample before the first elongation, and R was the resistance in course of the elongation; Ɛ represented the percentage of the mechanical strain, which was a relative change in length defined as $Ɛ = \Delta L/L_0$, where ΔL denoted the change in the specimen length and L_0 was the initial length before the first elongation. The periods of extension/relaxation were 120 s. The pre-strain composites were prepared by an initial extension of 14 % lasting for 10 min.

The relative resistance change increased with the strain deformation, **Fig. 6**. In addition, the increasing stress increased the residua of the relative resistance change, which remained after the cessation of the stress. The initial resistance mechanisms of both CNW and MWCNT networks were affected by an extension. The phenomenon has been adequately analyzed in our papers on the MWCNT/TPU composites **[19,20]**. As the SEM micrographs suggest, the resistance mechanism includes cracking of the composite network and consequently a decrease in many contacts between the carbon nanotubes. Thus, the network has fewer interconnections to carry the electric current. Nevertheless, the composite was conductive all the time, since network cracks were still bridged over by individual nanotubes. When the stress was released, the cracks contracted, and the number of intertube contacts increased, which restored the composite conductivity. As far as the resistance mechanism of the CNW/TPU composite in the stress test is concerned, SEM micrographs in **Fig. 4** and published results on the resistance change in a CNW/poly-dimethylsiloxane composite likewise suggest a role of the composite cracking **[1]**.

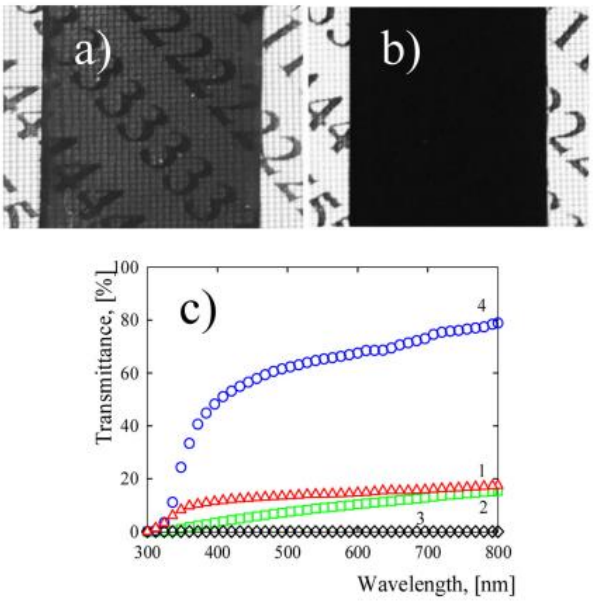

Fig. 5. a) Photo of the transparent CNW/TPU composite and b) the non-transparent MWCNT/TPU composite. Composite strips of thickness 1 mm were laid on a transparent PET foil with laser printed numbers and a grid. c) Transmittance spectra for the CNW/TPU composite attached to the TPU foil of 0.35 mm and 2 mm are numbered 1 (triangles) and 2 (squares), respectively. Transmittance spectra forthe MWCNT/TPU composite and TPU are numbered 3 (diamonds) and 4 (circles), respectively.

Likewise, the possible decrease and increase of intertube contacts during MWCNT/TPU extension/relaxation tests, a similar mechanism as discussed in **[1]** may explain the resistance changes in the CNW/TPU composite. That is, the resistance increase of extended CNW/TPU composite was due to widened cracks and the stretched CNW/TPU strings bridging the cracks. The relaxed phase of the test was then characterized by the resistance decrease through the closed cracks and hence, the growing number of contacts between carbon nanowalls. The repeated extension/relaxation cycles did not monitor any changes for which the supposed underlying resistance mechanism would be responsible. Moreover, when an initial pre-strain was applied to deform the CNW/TPU and MWCNT/TPU composites before the actual stepwise strain increase, the residual resistance was nearly constant, and the resistance response was increased, **Fig. 6**b. This impact can be explained by widening and closing of the pre-formed cracks (see **Fig. 4**c, d). Moreover, some contacts between either CNWs or MWCNTs were probably lost due to the pre-strain cracks, which increased the resistance values ofthe pre-strained composites in comparison with the not pre-strained composites.

A comparison of the relative resistance changes of three different CNW/TPU composites subjected to a sinusoidal strain, which varied cyclically between 0 and ~ 6.5 % with the frequency 0.046 Hz, is shown in **Fig. 7**a. The average distances of embedded nanowalls are indicated in the figure. Measurements were taken after a prestrain 14 % lasting 10 min. The resistance increase was highest for the composite with the average nanowall distance 300 nm. Precisely, the peak of the relative resistance changes in the CNW/TPU composites with the average nanowall distances 100, 200 and 300 nm was 60,150 and 312 %, respectively.

When comparing the waveform output of the MWCNT/TPU composite in **Fig. 7**b with the waveforms in **Fig. 7**a, the resistance change increase was faster than the rise of the strain value. However, the response of the MWCNT/TPU composite in terms of the relative resistance change was smaller than

in the case of the composites with CNWs with the average distances of nano walls 200 and 300 nm. The nanowalls lost contacts with each other more easily than the entangled nanotubes. On the other hand, a readjustment of the nanotube network and a formation of nanotube interconnects with decreasing strain were slower than in the case of the composite with embedded CNWs, which resulted in a deceleration of the resistance change decrease compared to the strain decrease.

To assess the stability of the CNW/TPU and MWCNT/TPU composites during the time-dependent resistance changes, the composites were likewise subjected to long-lasting strain cycles. The frequency of the cycles was ~ 0.7 Hz, and 1250 cycles for 30 min. were monitored. The applied strain varied between 0 and 6.5 %. The typical results showed that the resistance change was reproducible, and no irreversible changes of the composite were observed (**Fig. 8**a, cracked CNW and MWCNT networks stayed unaffected regardless of the number of deformation cycles. This reasonable stability of the resistance waveforms would be beneficial for potential practical applications.

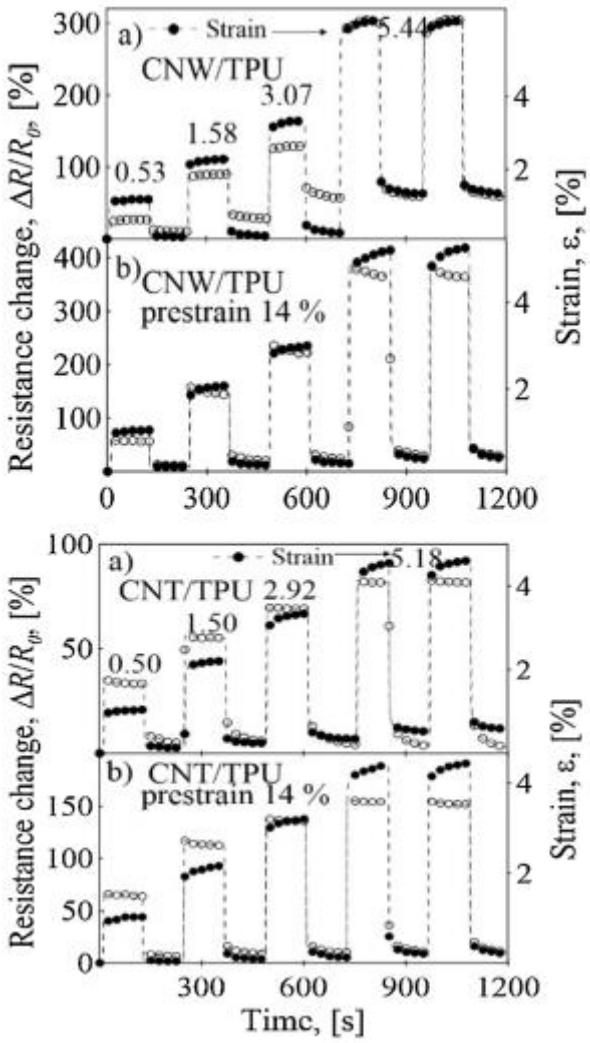

Fig. 6. Time-dependent response of the relative resistance change $\Delta R/R_0$ and strain Ɛ to the step increase of tensile stress in each of five cycles for the CNW/TPU and MWCNT/TPU composites. a), c) No pre-strain applied, b), d) pre-strain 14 %. The strain values are denoted by solid circles, the relative resistance change by open circles.

Responses of the CNW/TPU composite during an augmented frequency deformation were assessed by a measurement of the resistance change of the composite strips attached to a TPU strip (length 40 mm, width 10 mm and thickness 2 mm) anchored tightly on one side during a bending deformation induced by a tip deflection (15 mm) of its free ending, **Fig. 9.** Alike the response to the lower frequency deformation (**Fig. 7**a), the response to the high-frequency deformation was highest in terms of the relative resistance change in the composite with the average nanowall distance 300 nm.

According to the manufacturer (Bayer MaterialScience), the ultimate tensile strength ofTPU is 48.9 MPa and the strain at break is 442.2 %. Consequently, it was tested if the embedding CNWs or MWCNTs into this highly elastic polymer would not change its elastic properties and strain at break. Both the CNW/TPU (average nanowall distance 100 nm) and MWCNT/TPU composites were stretchable as well as electrically conductive until the TPU fracture strain was reached (**Fig. 10**a). The observed increase in the resistance change with strain was continuous. The CNW and MWCNT network cracks were bridged over by conductive nanowall strings or nanotubes during extension phases up until the fracture strain was reached.

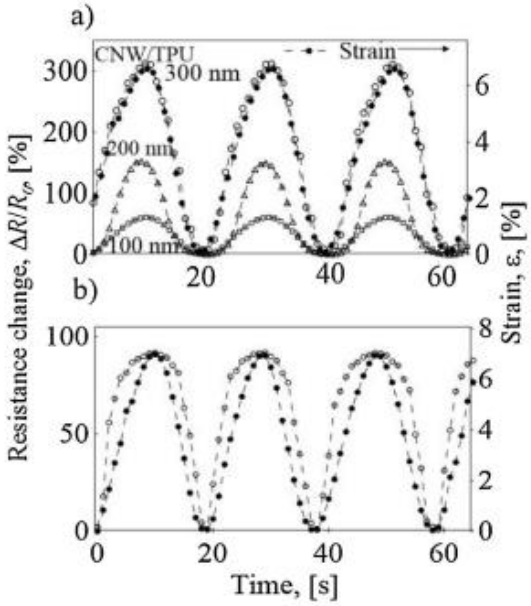

Fig. 7. a) Relative resistance change of the CNW/TPU composites with the average distance of embedded nanowalls 100, 200 and 300 nm during strain cycles (0-6.5 %) with the frequency 0.046 Hz and the initial pre-strain 14 %. The strain values are denoted by solid circles, the relative resistance change by open circles. b) Relative resistance changes ofthe MWCNT/TPU composite during strain cycles (0-6.5 %) with the frequency 0.046 Hz and the initial pre-strain 14 %. The strain values are denoted by solid circles, the relative resistance change by open circles.

The sensitivity to the strain of electrically conductive materials is usually expressed quantitatively as a gauge factor, which is defined as the relative resistance change versus the applied strain Ɛ, GF=($\Delta R/R_0$)/Ɛ. To have a high sensitivity, that is, a great change in the resistance for the same strain, a higher value of the gauge factor is desirable. Whereas metal foil strain gauges have GF of 2-5, the gauge factor of strain sensors with carbon nanotubes in polymeric matrices ranges 200-500 **[21]**. In comparison to the gauge factor values of such MWCNT/polymer composites, the gauge factor and thus sensitivity of the CNW/TPU composite was nearly an order of magnitude greater reaching GF of 2000,

Fig. 10b. Consequently, the CNW/TPU composite strain sensors have the potential to replace the ones with embedded MWCNTs used in many advanced applications **[22]**.

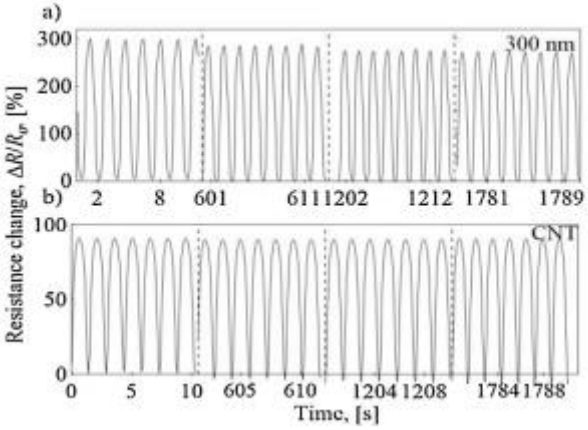

Fig. 8. a) Test ofthe pre-strained (14%) CNW/TPU composite (average nanowall distance 300 nm) subjected to more than 1000 strain cycles (0-6.5 %). The frequency of strain variation was ~0.7 Hz. b) Test ofthe pre-strained (14 %) MWCNT/TPU composite subjected to more than 1000 strain cycles (0-6.5 %). The frequency of the strain variation was again ~0.7 Hz.

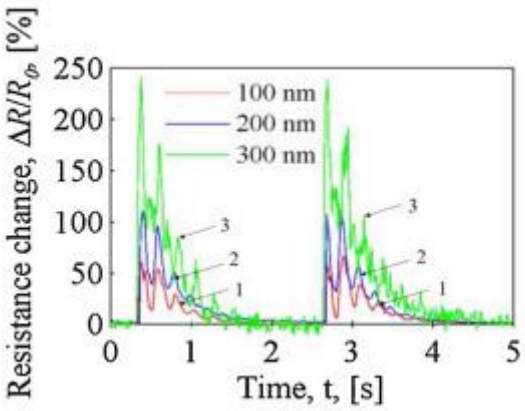

Fig. 9. Time-dependent relative resistance changes response of the cantilevered strip ofthe CNW/TPU composite with the average distance of embedded nanowalls 100 (curve no. 1), 200 (curve no. 2) and300 nm (curve no. 3)to a rapid deflection of its loose end.

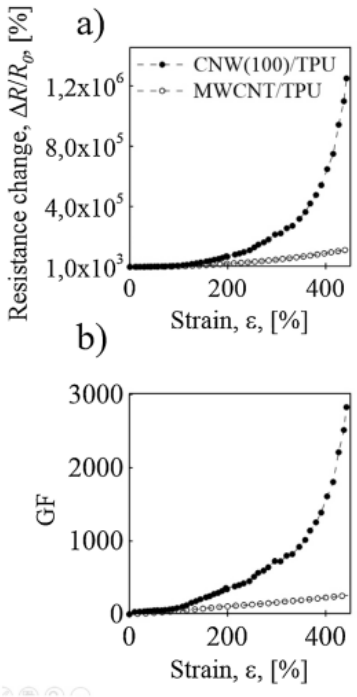

Fig. 10. a) Strain dependence ofthe relative resistance change ofthe CNW/TPU and MWCNT/PU composites until the fracture strain. b) Strain dependence of the gauge factor (GF) of CNW/TPU and MWCNT/PU composites until the fracture strain.

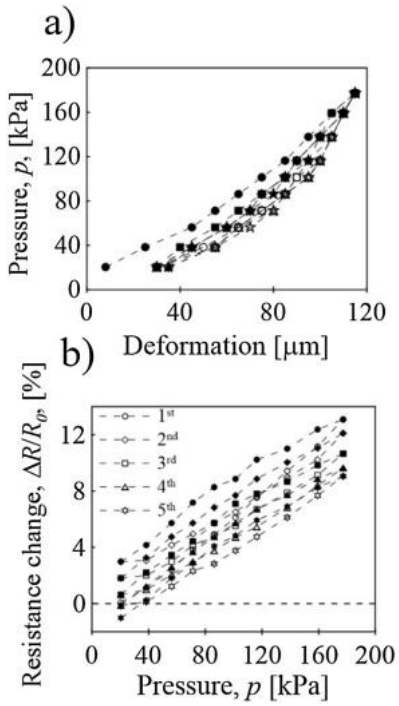

Fig. 11. The composite strip deformation and resistance change during five com-pression/relaxation cycles of the CNW/TPU composite. The full symbols and open symbols denote the resistance change with the increasing and decreasing pressure, respectively. a) Dependence of pressure on the CNW/TPU composite deformation by a steel plate. The inset numbers in b) denotes the cycle order.

The change of the relative resistance of the CNW/TPU composite with the average nanowall distance 300 nm was also measured in the course of five compression/relaxation cycles, **Fig. 11**. The results plotted as the resistance change vs. pressure are presented in **Fig. 11**b. The resistance change at the end of the first cycle was about 13 % at applied compression 177.2 kPa. The resistance change decreased after the first cycle as well as after the next ones.

These irreversible changes and hysteresis were observed owing to possible compaction of nanowall layers, which may increase the number and conductivity of nano wall contacts. The acting pressure did not induce a sufficient composite extension in the direction perpendicular to the direction of compression (Poisson effect) to disrupt the nanowall network by cracks. This was different to the resistance change of the MWCNT/TPU composites, in which cracks are formed due to compression since the pressure required for corresponding resistance changes is two orders of magnitude higher than in case of the CNW/TPU composites **[23]**. Consequently, the CNW/TPU composites can monitor much lower pressures, which the MWCNT/TPU composites cannot detect.

As an example of practical use of the CNW/TPU composite for wearable applications, the composite was attached to a finger of a glove and used to detect flexion of a finger, **Fig. 12**. This flexion of the finger was identified by a resistance change of the composite. Generally, the wearable strain sensors may be useful in orthopaedics and rehabilitation.

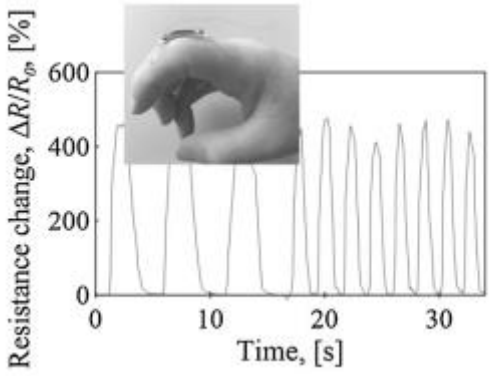

Fig. 12. Relative resistance changes of the CNW/TPU composite with the average nanowall distance 300 nm resulting from the finger bending.

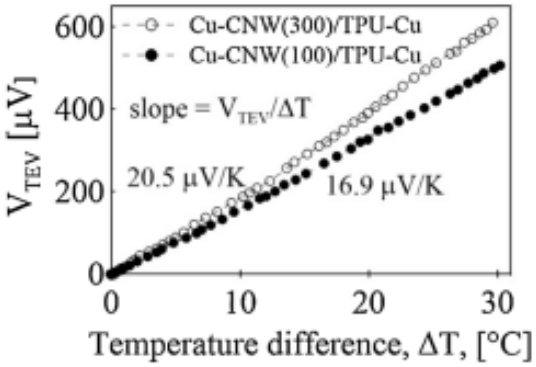

Fig. 13. Generated voltage vs. temperature difference forthe CNW/TPU composites with the average nanowall distance 100 and 300 nm together with the indicated thermoelectric power $S = V_{TEV}/\Delta T$ in μV/K at room temperature.

Fig. 13 shows the values of the induced voltage in response to a temperature difference across thermoelectric CNW/TPU composites. The slope of the linear temperature difference AT dependence on the resulting voltage V_{TEV} defines the thermoelectric power $S = V_{TEV} / \Delta T$, an essential measure for evaluating a potential thermoelectric performance. The corresponding thermoelectric power was 16.9 and 20.5 μV/K for the CNW/TPU composites with the average nanowall distance 100 and 300 nm, respectively. Those thermoelectric power values are either higher or comparable to the corresponding values of some metallic thermoelectrics, e.g., Al, Ag, Cu, Sb, chromel, alumel. Despite that, the carbon allotrope/TPU composite thermoelectric power factor $S^2\sigma$, which is directly related to the usable power attainable from the thermoelectric materials, is still lower than the ones of metals. The reason for that is that the electrical conductivity σ of carbon allotrope/TPU composites, in comparison with the ones of metals, is about one order lower. Regardless of this disadvantage, the mechanical flexibility, processability, light weight and low manufacturing costs of CNT/TPU composites may be more desirable and looked for in appropriate applications than costly, heavy and materially in short supply metallic thermoelectrics.

From the presented results comparing the selected CNW/TPU and MWCNT/TPU properties followed a prevailing better performance of the CNW/TPU composites than the MWCNT/TPU composites in terms of a higher resistance change in the course of extension/relaxation cycles both with and without pre-strain history as well as in the extension deformation until the fracture strain. Although both CNW/TPU and MWCNT/TPU composites were stretchable and electrically conductive until the fracture strain (440 %), the difference between the relative resistance changes and extension detection sensitivities were substantial. The resistance changes and the extension detection sensitivity at the maximum extension was in the CNW/TPU composite (average nanowall distance 100 nm) about 46 times higher than in the corresponding MWCNT/TPU composite.

4. Conclusions

We introduced highly deformable composites comprising of a vertically aligned network of electrically conductive CNWs embedded in an elastic polyurethane into which CNWs were transferred from a rigid technological layered substrate. Results of multiple tests of the new type of composites confirmed that they had many favorable properties. While these composites could be highly extended as much as 400 % they retain a high sensitivity to strain. Their extension detection sensitivity evaluated by the gauge factor increased over two thousand, which was exceptional and thus ranked the CNW/TPU composites among materials with the highest electromechanical sensitivity. The revealed properties of the CNW/TPU composites indicate the potential of these composites to replace the MWCNT/TPU composites in strain monitoring applications. Moreover, both an extension and compression can be measured by one sensor made from this CNW/TPU composite. Altogether, the CNW/TPU composites offered properties, which can be applied, e.g., in extension and pressure sensors, wearable sensors for human motion detection, etc. The combination of strain sensing and thermoelectrical properties of the CNW/TPU composites may be advantageous in an application where a source of waste heat could supply electricity to detect the expansivity of the monitored components.

References

[1] S. Wu, S. Peng, Z.J. Han, H. Zhu, C.H. Wang, Ultrasensitive and stretchable strain sensors based on mazelike vertical graphene network, ACS Appl. Mater. Interfaces 10 (2018) 36312-36322, http://dx.doi.org/10.1021/acsami. 8b15848.

[2] Z. Feng, S. Rafique, Y. Cai, L. Han, M.-C. Huang, H. Zhao, ZnO nanowall networks for sensor devices: from hydrothermal synthesis to device demonstration, ECS J. Solid State Sci. Technol. 7 (2018) Q3114-Q3119, http:// dx.doi.org/10.1149/2.0221807jss.

[3] J. Yang, D. Wei, L. Tang, X. Song, W. Luo, J. Chu, T. Gao, H. Shi, C. Du, Wearable temperature sensor on graphene nanowalls, RSC Adv. 5 (2015) 25609-25615, http://dx.doi.org/10.1039/C5RA00871A.

[4] M. Tomatsu, M. Hiramatsu, J.S. Foord, H. Kondo, K. Ishikawa, M. Sekine, K. Takeda, M. Hori, Hydrogen peroxide sensor based on carbon nanowalls grown by plasma-enhanced chemical vapor deposition,Jap.J. Appl. Phys. 56 (2017), 06HF03, http://dx.doi.org/10.7567/JJAP.56.06HF03.

[5] Q. Chen, T. Sun, X. Song, Q. Ran, C. Yu,J. Yang, H. Feng, L. Yu, D. Wei, Flexible electrochemical biosensors based on graphene nanowalls for the real-time measurement oflactate, Nanotechnology 28 (217) (2017), 315501, http://dx. doi.org/10.1088/1361-6528/aa78bc.

[6] I. Tzouvadaki, N. Aliakbarinodehi, D.D. Pineda, G. De Micheli, S. Carrara, Graphene nanowalls for high-performance chemotherapeutic drug sensing and anti-fouling properties, Sens. Actuator B-Chem. 262 (2018) 395-403, http://dx.doi.org/10.1016Zj.snb.2018.02.036.

[7] E. Luais, M. Boujtita, A. Gohier, A. Tailleur, S. Casimirius, M.A. Djouadi, A. Granier, P.Y. Tessier, Carbon nanowalls as material forelectrochemical transducers, Appl. Phys. Lett. 95 (2009), 014104, http://dx.doi.org/10.1063/1. 3170033.

[8] M. Hiramatsu, S. Mitsuguchi,T. Horibe, H. Kondo, M. Hori, H. Kano, Fabrication ofcarbon nanowalls on carbon fiber paper for fuel cell application,Jap.J. Appl. Phys. 52 (2013), 01AK03, http://dx.doi.org/10.7567/JJAP.52.01AK03.

[9] J. Yang, Q. Ran, D.P. Wei, T. Sun, L.Y. Yu, X.F. Song, L.C. Pu, H.F. Shi, C.L. Du, Three-dimensional conformal graphene microstructure for flexible and highly sensitive electronic skin, Nanotechnology 28 (2017) 115501, http://dx.doi. org/10.1088/13616528/aa5b56.

[10] N. Soin, S.S. Roy, C. O'Kane,J.A.D. McLaughlin, T.H. Limb, C.J.D. Hetherington, Exploring the fundamental effects ofdeposition time on the microstructure of graphene nanoflakes by Raman scattering and X-ray diffraction, Cryst. Eng. Comm. 13 (2011)312-318, http://dx.doi.org/10.1039/C0CE00285B.

[11] H.J. Cho, H. Kondo, K. Ishikawa, M. Sekine, M. Hiramatsu, M. Hori, Density control ofcarbon nanowalls grown by CH4/H2 plasma and their electrical properties, Carbon 68 (2014) 380-388, http://dx.doi.org/10.1016/j.carbon. 2013.11.014.

[12] Y.H. Wu, P.W. Qiao, T.C. Chong, Z.X. Shen, Carbon nanowalls grown by microwave plasma enhanced chemical vapor deposition, Adv. Mater. 14 (2002) 64-67, http://dx.doi.org/10.1002/1521-4095(20020104)14:1.

[13] D.H. Seo, S. Kumar, K. Ostrikov, Control of morphology and electrical properties of self-organized graphenes in a plasma, Carbon 49 (2011) 4331-4339, http://dx.doi.org/10.1016/j.carbon.2011.06.004.

[14] W. Takeuchi, M. Ura, M. Hiramatsu, Y. Tokuda, H. Kano, M. Hori, Electrical conduction control of carbon nanowalls, Appl. Phys. Lett. 92 (2008), 213103, http://dx.doi.org/10.1063/1.2936850.

[15] Z.H. Wu, B.J. Yang, B.Y. Zong, H. Sun, Z.X. Shen, Y.P. Feng, Carbon nanowalls and related materials,J. Mat. Chem. 14 (2004) 469-477, http://dx.doi.org/10. 1039/B311682D.

[16] P. Slobodian, U. Cvelbar, P. Riha, R. Olejnik, J. Matyas, G. Filipic, H. Watanabe, S. Tajima, H. Kondo, M. Sekine, M. Hori, High sensitivity of a carbon nanowall-based sensor for detection oforganic vapours, RSC Adv. 5 (2015) 90515-90520, http://dx.doi.org/10.1039/C5RA12000D.

[17] X. Zhou, Y. Zhang, J. Yang, J. Li, S. Luo, D. Wei, Flexible and highly sensitive pressure sensor based on microstructured carbon nanowalls electrodes, Nanomaterials 9 (2019) 496-506, http://dx.doi.org/10.3390/nano9040496.

[18] P. Slobodian, P. Riha, A. Lengalova, P. Saha, Compressive stress-electrical conductivity characteristics ofmultiwall carbon nanotube networks, J. Mat. Sci. 46(2011)3186-3190, http://dx.doi.org/10.1007/s10853-010-5202-0.

[19] P. Slobodian, P. Riha, P. Saha, A highly-deformable composite composed ofan entangled network ofelectrically-conductive carbon-nanotubes embedded in elastic polyurethane, Carbon 50 (2012) 3446-3453, http://dx.doi.org/10. 1016/j.carbon.2012.03.008.

[20] P. Slobodian, P. Riha, R. Olejnik, U. Cvelbar, P. Saha, Enhancing effect ofKMnO4 oxidation ofcarbon nanotubes network embedded in elastic polyurethane on overall electro-mechanical properties of composite, Compos. Sci. Technol. 81 (2013) 54-60, http://dx.doi.org/10.1016/j.compscitech.2013.03.023.

[21] J.L. Abot, et al., Foil Strain gauges using piezoresistive carbon nanotube yarn: fabrication and calibration, Sensors 18 (2018) 464, http://dx.doi.org/10.3390/ s18020464.

[22] H. Peng, Q. Lin, T. Chen, Industrial Applications ofCarbon Nanotubes, Elsevier, New York, 2017, Chpts 5, 7.

[23] P. Slobodian, P. Riha, R.Olejnik,J. Matyas, M. Kovar, Poisson effect enhances compression force sensing with oxidized carbon nanotube network/polyurethane sensor, Sens. Actuator A-Phys. 271 (2018) 76-82, http://dx.doi.org/10.1016/j.sna.2017.12.035.